Since January 2020 Elsevier has created a COVID-19 resource centre with free information in English and Mandarin on the novel coronavirus COVID-19. The COVID-19 resource centre is hosted on Elsevier Connect, the company's public news and information website.

Partial Differential Equations in Applied Mathematics 5 (2022) 100212

Contents lists available at ScienceDirect

Partial Differential Equations in Applied Mathematics

journal homepage: www.elsevier.com/locate/padiff

Mathematical modelling of COVID-19 transmission dynamics in a partially comorbid community

J. Ssebuliba [a,*], J.N. Nakakawa [a], A. Ssematimba [b], J.Y.T. Mugisha [a]

[a] Department of Mathematics, School of Physical Sciences, College of Natural Science, Makerere University, P.O. Box 7062, Kampala, Uganda
[b] Department of Mathematics, Faculty of Science, Gulu University, P.O. Box 166, Gulu, Uganda

ARTICLE INFO

Keywords:
Mathematical modelling
COVID-19
Comorbidity
Community transmission

ABSTRACT

A deterministic $S, E_m, E_c, I_m, I_c, H, R$ epidemic model that describes the spreading of SARS-COV-2 within a community with comorbidities is formulated. Size dependent area is incorporated into the model to quantify the effect of social distancing and the results indicate that the risk of community transmission is optimally minimised when the occupancy area is increased. The reproduction number is shown to have a positive relationship with the infection rate, the proportion of individuals with comorbidities and the proportion of susceptible individuals adhering to standard operating procedures. The model exhibits a unique endemic equilibrium whose stability largely depends on the rate of hospitalisation of individuals with underlying health conditions (ω_m) as compared to those without these conditions (ω_c), such that stability is guaranteed if $\omega_m < \omega_c$. Furthermore, if individuals with comorbidities effectively report for treatment and hospitalisation at a rate of 0.5 per day, the epidemic curve peaks 3-fold higher among people with comorbidities. The infection peaks are delayed if the area occupied by community is increased. In conclusion, we observed that community infections increase significantly with decreasing detection rates for both individuals with or without comorbidities.

1. Introduction

Since the reporting of its first case in December 2019, Corona virus Disease (COVID-19) has had a significant impact on global public health with over 246 million reported cases and more than 4.9 million deaths as of October 2021 coupled with an imaginable economic devastation.[1] In some countries, as hospitals run out of patient admission facilities, disease severity is being considered among the factors to decide on whether or not to admit a patient. This criteria calls for the evaluation of intervention scenarios with special consideration for the vulnerable people such as the elderly and the comorbid individuals.

For COVID-19, it can be concluded based on clinical observations and studies that among infected individuals, adverse clinical outcomes such as case severity and mortality seem to vary regionally and also vary within a given population. The elderly and comorbid individuals seem to be the most vulnerable to severe outcomes of COVID-19. This variation is likely due to differences in immune response capacity related to age and the presence of medical comorbidities and pre-existing conditions that may exert pressure on the immune system.[2] There are reports of a strong link between severe and/or fatal COVID-19 and other communicable or non-communicable diseases and such as age and risk factors such as smoking, exposure to polluted air.

The relationship between comorbidities and disease severity seems to have been observed globally. For example, Ye et al.,[3] studied the hospitalisation data for Zhejiang Province in China and reported that COVID-19 patients with comorbidities had worse clinical outcomes. The study also revealed that extreme and serious manifestations of adverse outcomes were positively correlated with the number of comorbidities the patient suffered from. Older obese patients were reported to experience more severe clinical outcomes.[4] Comorbidities such as diabetes,[5,6] hypertension, cardiovascular disease,[7] chronic lung disease, tuberculosis[8] and the malnourished and those with HIV[2] were all reported to be more affected. For example, the incidences of hypertension, cardio-cerebrovascular diseases, and diabetes mellitus were 2-3-fold higher in intensive care unit (ICU)/severe cases than in their non-ICU/severe counterparts.[7]

In a French study of 124 consecutive hospitalised COVID-19 patients, obesity and severe obesity were present in 47.6% and 28.2% of cases, respectively[9] and for the United States, Thomas et al.[10] reported approximately 42% as being obese of whom 85% had type 2 diabetes. Another modelling study with comorbidities parameterised using data from Nigeria[11,12] showed that the top ranked parameters that drive the dynamics of the co-infection model were the effective contact rate for COVID-19 transmission, the parameter accounting for increased susceptibility to COVID-19 by comorbid susceptibles, the comorbidity development rate, the detection rate for singly infected and co-infected individuals, as well as the recovery rate from COVID-19 for co-infected individuals.

* Corresponding author.
E-mail address: joseph.ssebuliba@mak.ac.ug (J. Ssebuliba).

https://doi.org/10.1016/j.padiff.2021.100212
Received 30 March 2021; Received in revised form 10 November 2021; Accepted 10 November 2021

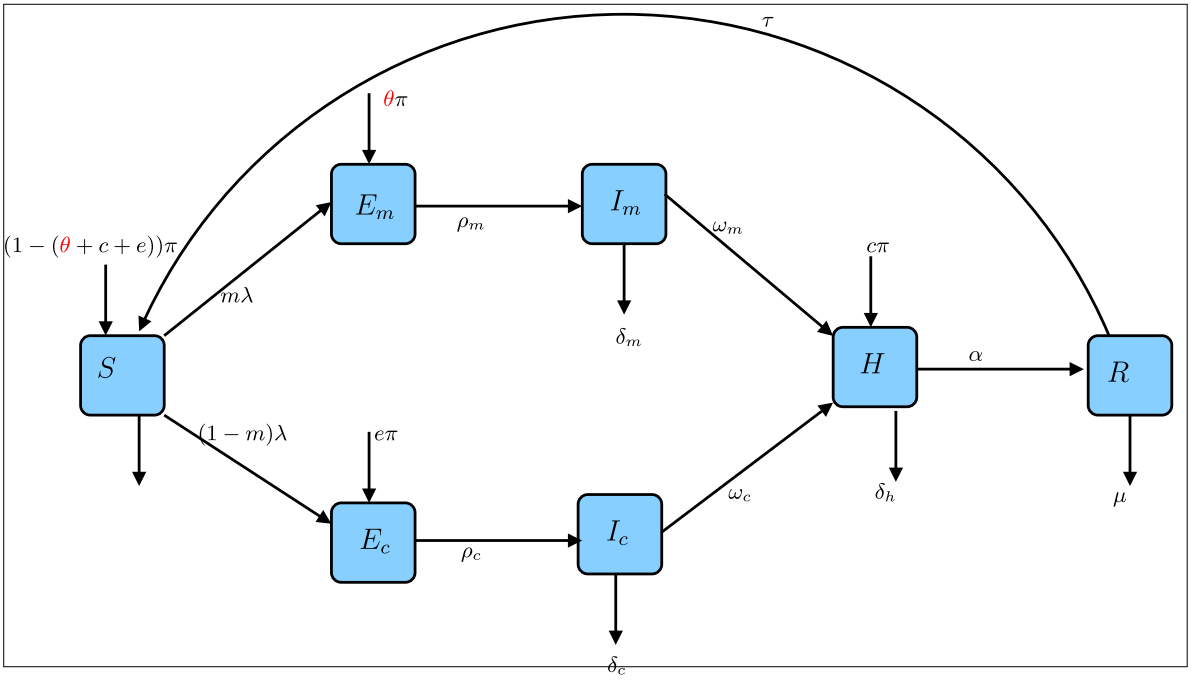

Fig. 1. Schematic diagram for COVID-19 co-morbidity disease dynamics.

Enhancing the overall efficiency of the public health responses, requires a thorough understanding of the impact of COVID-19 on these comorbidities and mathematical modelling permits evaluation of various comorbidity and age-dependence scenarios on disease dynamics. Modelling comorbidity is not only seen from the perspective of the dynamics of re-infection and co-infection with comorbidities, but may be more to do with the impacts of the comorbidities on the severity of COVID-19. It is well observed that individuals with underlying health conditions are more likely to report to health facilities than those without comorbidities. There is therefore high chance of persons without comorbidities likely to remain in communities spreading the infection as compared to persons with comorbidities.

Many aspects of the dynamics of COVID-19 are built on pre-existing health conditions and adherence to standard operating procedures (SoPs). Models that can provide insights on how individuals with compromised health conditions are affected by COVID-19, need to be developed to help in designing effective mitigation and intervention strategies. Furthermore, size dependent area has been incorporated into the model in order to measure the effectiveness of social distancing. Therefore, a mathematical model has been developed to ascertain how COVID-19 dynamics impacts underlying comorbidities, and then used to investigate how early detection and reporting for treatment benefits the overwhelmed health facilities, consequently minimising community transmissions.

2. Model formulation

2.1. Model description

In this section, we present a model for the transmission dynamics of COVID-19 amongst a population with a proportion of individuals having underlying comorbidities. We consider the entire population to be susceptible $S(t)$ and when infected with COVID-19, they are classified as exposed individuals with comorbidities ($E_m(t)$) or without comorbidities ($E_c(t)$). Individuals will then progress to the infectious classes ($I_m(t)$) and $I_c(t)$ respectively depending on their comorbidity status. Individuals in the $I_m(t)$ and $I_c(t)$ will either by contact tracing or self reporting join the hospitalised class ($H(t)$) . Recovered individuals from hospitals are grouped in the $R(t)$ class.

The transition process is as follows: Susceptible individuals get infected through contact with an infected person. Once infected, depending on their co-morbidity status, a proportion m will join the $E_m(t)$ while the remaining proportion will be grouped in the $E_c(t)$ class. After a given latent period, latently infected individuals will progress to the $I_m(t)$ and $I_c(t)$ classes at rates ρ_m and ρ_c respectively. Due to the underlying conditions of individuals in the $E_m(t)$ compartment, it is assumed that $\rho_c < \rho_m$. To explicitly capture and highlight the impact of comorbidities, we assume similar characteristics for asymptomatic and symptomatic and divide infected class into $I_c(t)$ and $I_m(t)$. Individual in the $I_m(t)$ and $I_c(t)$ classes may be traced and hospitalised or do self reporting at rates ω_m and ω_c respectively. It is assumed that those in the $I_m(t)$ class are likely to do self reporting much easier given their status as compared to those in the $I_c(t)$ class. It is assumed that the disease related mortality rates will vary depending on whether the infected individual has a co-morbidity. The disease related mortality rate for individuals in $I_m(t)$ class is considered to be δ_m while that of individuals in the $I_c(t)$ is given as δ_c. Hospitalised individuals may recover from COVID-19 at a rate α or die at a rate δ_h. The recovered individuals have temporary disease induced immunity[11] which wanes off and they become susceptible again at a rate τ.

The model captures entry of individuals at a constant rate π of which a proportion θ being latently infected with a co-morbidity, e latently infected without co-morbidity, c being a proportion of those that are confirmed to be infected at the entry points and immediately hospitalised and the rest being susceptible. Susceptible and recovered individual exit the community at a per-capita rate μ.

To model COVID-19 transmission, we consider an area-dependent force of infection term given as $\big(\beta bS(I_c + I_m + gH)\big)/A$ where β is the transmission rate and b is proportion of susceptible individuals that do not adhere to standard operating procedures, g is the percent reduction of hospital acquired infections and A is the total area occupied by the given community.

2.2. Model equations

Taking into account the above description, along with the dynamics as in Fig. 1, gives the model system as;

$$\frac{dS}{dt} = (1-(\theta+c+e))\pi - \frac{\beta bS(I_m + I_c + gH)}{A} - \mu S + \tau R,$$

$$\begin{aligned}
\frac{dE_m}{dt} &= \theta\pi + \frac{m\beta bS(I_m + I_c + gH)}{A} - \rho_m E_m,\\
\frac{dE_c}{dt} &= e\pi + \frac{(1-m)\beta bS(I_m + I_c + gH)}{A} - \rho_c E_c,\\
\frac{dI_m}{dt} &= \rho_m E_m - \delta_m I_m - \omega_m I_m,\\
\frac{dI_c}{dt} &= \rho_c E_c - \delta_c I_c - \omega_c I_c,\\
\frac{dH}{dt} &= c\pi + \omega_m I_m + \omega_c I_c - \delta_h H - \alpha H,\\
\frac{dR}{dt} &= \alpha H - \mu R - \tau R.
\end{aligned} \tag{2.1}$$

3. Mathematical analysis

We ascertain epidemiological feasibility of the model system (2.1), by guaranteeing that starting with non negative initial conditions, the solutions will remain non-negative for all $t \geq 0$. Consider the given initial conditions of system (2.1) ($S(0) \geq 0, E_m(0) \geq 0, E_c(0) \geq 0, I_m(0) \geq 0, I_c(0) \geq 0, H(0) \geq 0$ and $R(0) \geq 0$, then the resulting solutions, $(S(t), E_m(t), E_c(t), I_m(t), I_c(t), H(t), R(t))$, will remain non-negative for all $t \geq 0$.

To prove this, it is sufficient to show that all the trajectories of system (2.1) are non-negative for time $t > 0$. From the first equation of system (2.1), the evolution of susceptible individuals over time will be given by the inequality;

$$\frac{dS(t)}{dt} \geq -\left(\frac{\beta b\Big(I_m(t) + I_c(t) + gH(t)\Big)}{A} + \mu\right)S(t).$$

By solving the inequality and taking the limit as $t \to \infty$, we have

$$S(t) \geq S_0 \exp\left\{-\left(\mu t + \int_0^t \left(\frac{\beta b\Big(I_m(\tau) + I_c(\tau) + gH(\tau)\Big)}{A}\right)d\tau\right)\right\},$$

$$\liminf_{t\to\infty} S(t) \geq 0.$$

Similarly, it can be shown that $E_m(t) \geq 0, E_c(t), I_m(t) \geq 0, I_c(t) \geq 0, H(t) \geq 0$ and $R(t) \geq 0$. Hence all solutions of system (2.1) will remain non-negative whenever we have non-negative initial conditions.

It is also important to note that, the closed set $D = \left\{(S, E_m, E_c, I_m, I_c, H, R) \in \mathbb{R}^7_+; N \leq \frac{\pi}{\mu}\right\}$, is positively invariant and attracts all positive solutions of the model since

$$\begin{aligned}
\frac{dN}{dt} &= \pi - \mu(S+R) - \delta_c I_c - \delta_m I_m - \delta_h H,\\
&= \pi - \mu N, \quad \text{at disease free equilibrium.}
\end{aligned}$$

We observe that $N > \frac{\pi}{\mu}$ whenever $\frac{dN}{dt} < 0$. Since the right hand side of $\frac{dN}{dt}$ is always bounded, then by standard comparison Theorem,[13] it can be shown that $N(t) \leq N(0)e^{-\mu t} + \frac{\pi}{\mu}(1 - e^{-\mu t})$. Therefore $\limsup_{t\to\infty} N(t) = \frac{\pi}{\mu}$, implying that if $N(0) \leq \frac{\pi}{\mu}$, then $N(t) \leq \frac{\pi}{\mu}$. The domain D is positively invariant under the flow of system (2.1). Therefore, system (2.1) is biologically feasible and mathematically well posed in D.

3.1. Local stability of the disease free equilibrium and computation of $\mathcal{R}_0$

The model system (2.1) has a disease free equilibrium (ξ_0) given by $\xi_0 = (\pi/\mu, 0, 0, 0, 0, 0, 0)$. Using the next generation matrix described by van den Driessche and Watmough,[14] the local stability of ξ_0 is investigated. The basic reproduction number, $\mathcal{R}_0$ (defined as the average number of secondary infections generated by COVID-19 infectious individuals through out their infectious period if introduced into a population with a proportion of individuals having a comorbidity) is also determined by the same method. Let $\mathcal{F}$ denote the rate of appearance of new infections into the infected compartments and $\mathcal{V}$ the transfer in and out of the infected compartments. We obtain the derivatives of the matrix $\mathcal{F}$ and $\mathcal{V}$ evaluated at ξ_0 and the obtained results are as given in Box I. The spectral radius, ρ, of matrix FV^{-1} gives the reproduction number as,

$$\mathcal{R}_0 = \rho(FV^{-1}) = \mathcal{R}_{I_m} + \mathcal{R}_{I_c},$$

where $\mathcal{R}_{I_m} = \frac{b\beta m\pi\left(\alpha + g\omega_m + \delta_h\right)}{A\mu\left(\delta_m + \omega_m\right)\left(\alpha + \delta_h\right)}$, $\mathcal{R}_{I_c} = \frac{b\beta(1-m)\pi\left(\alpha + g\omega_c + \delta_h\right)}{A\mu\left(\alpha + \delta_h\right)\left(\delta_c + \omega_c\right)}$.

The threshold quantity $\mathcal{R}_0$ is the basic reproduction of the model system (2.1). It measures the number of new COVID-19 cases that are generated by an infectious individual introduced into a population with a fraction of individuals having other comorbidities. It is given as the sum of the respective reproduction numbers associated with new cases generated by individuals without any comorbidity ($\mathcal{R}_{I_c}$) and those with any underlying comorbidity ($\mathcal{R}_{I_m}$). These threshold values are observed to have a positive relationship with the infection rate, proportion of susceptible individuals adhering to Standard operating Procedures (SOPs) and a negative relationship with the habitat area size.

The constituent reproduction number $\mathcal{R}_{I_m}$ ($\mathcal{R}_{I_c}$) can be interpreted as the product of effective transmission rate, proportion of individuals adhering to SOPs, proportion of individuals with (without) comorbidities, time taken for a COVID-19 infected individual with (without) comorbidity to report to hospital and the time it takes a hospitalised individual to succumb or recover from COVID-19. Using the result of Driessche and Watmough[14] in Theorem 2, the following lemma is established.

Lemma 3.1. *The DFE, ξ_0 of model system (2.1), is locally asymptotically stable if $\mathcal{R}_0 < 1$ and unstable if $\mathcal{R}_0 > 1$.*

Lemma 3.1 epidemiologically indicates that if a small number of COVID-19 infectives are introduced into a community where a fraction of individuals are having comorbidities, then the resulting number of secondary cases will not lead to an outbreak whenever $\mathcal{R}_0 < 1$. But if $\mathcal{R}_0 > 1$, then the number of cases in the subsequent generation will be greater than the former and as a result the disease will spread and become endemic in the community. In this case the disease will continue to spread until the proportion of susceptible individuals is too small such that the probability of infecting a new person is very low. To ensure that elimination of the virus from the population is independent of the initial population size, we investigate the global stability of the disease free equilibrium.

3.2. Global stability of disease free equilibrium

Theorem 3.1. *The DFE, ξ_0, of the model system (2.1), is globally asymptotically stable in the invariant region D if $\mathcal{R}_0 < 1$ and unstable if $\mathcal{R}_0 > 1$.*

Proof. Consider the positively definite Lyapunov function,

$$\begin{aligned}
L = &\frac{\left(\alpha + g\omega_m + \delta_h\right)E_m}{g\left(\delta_m + \omega_m\right)\left(\alpha + \delta_h\right)} + \frac{\left(\alpha + g\omega_c + \delta_h\right)E_c}{g\left(\alpha + \delta_h\right)\left(\delta_c + \omega_c\right)}\\
&+ \frac{\left(\alpha + g\omega_m + \delta_h\right)I_m}{g\left(\delta_m + \omega_m\right)\left(\alpha + \delta_h\right)} + \frac{\left(\alpha + g\omega_c + \delta_h\right)I_c}{g\left(\alpha + \delta_h\right)\left(\delta_c + \omega_c\right)} + \frac{dH}{\alpha + \delta_h}.
\end{aligned} \tag{3.1}$$

The time-derivative of function (3.1) is given by,

$$\begin{aligned}
\frac{dL}{dt} = &\frac{\left(\alpha + g\omega_m + \delta_h\right)}{g\left(\delta_m + \omega_m\right)\left(\alpha + \delta_h\right)}\frac{dE_m}{dt}\\
&+ \frac{\left(\alpha + g\omega_c + \delta_h\right)}{g\left(\alpha + \delta_h\right)\left(\delta_c + \omega_c\right)}\frac{dE_c}{dt} + \frac{\left(\alpha + g\omega_m + \delta_h\right)}{g\left(\delta_m + \omega_m\right)\left(\alpha + \delta_h\right)}\frac{dI_m}{dt}\\
&+ \frac{\left(\alpha + g\omega_c + \delta_h\right)}{g\left(\alpha + \delta_h\right)\left(\delta_c + \omega_c\right)}\frac{dI_c}{dt} + \frac{dH}{\alpha + \delta_h},
\end{aligned}$$

$$F = \begin{pmatrix} 0 & 0 & \frac{b\beta m\pi}{A\mu} & \frac{b\beta m\pi}{A\mu} & \frac{b\beta g m\pi}{A\mu} \\ 0 & 0 & \frac{b\beta(1-m)\pi}{A\mu} & \frac{b\beta(1-m)\pi}{A\mu} & \frac{b\beta g(1-m)\pi}{A\mu} \\ 0 & 0 & 0 & 0 & 0 \\ 0 & 0 & 0 & 0 & 0 \\ 0 & 0 & 0 & 0 & 0 \end{pmatrix}, \quad V = \begin{pmatrix} \rho_c & 0 & 0 & 0 & 0 \\ 0 & \rho & 0 & 0 & 0 \\ -\rho_m & 0 & \delta_m+\omega_m & 0 & 0 \\ 0 & -\rho_c & 0 & \delta_c+\omega_c & 0 \\ 0 & 0 & -\omega_m & -\omega_c & \alpha+\delta_h \end{pmatrix},$$

with

$$FV^{-1} = \begin{pmatrix} \frac{b\beta m\pi(\alpha+g\omega_m+\delta_h)}{A\mu(\delta_m+\omega_m)(\alpha+\delta_h)} & \frac{b\beta m\pi(\alpha+g\omega_c+\delta_h)}{A\mu(\alpha+\delta_h)(\delta_c+\omega_c)} & \frac{b\beta m\pi(\alpha+g\omega_m+\delta_h)}{A\mu(\delta_m+\omega_m)(\alpha+\delta_h)} & \frac{b\beta m\pi(\alpha+g\omega_c+\delta_h)}{A\mu(\alpha+\delta_h)(\delta_c+\omega_c)} & \frac{b\beta g m\pi}{A\mu(\alpha+\delta_h)} \\ \frac{b\beta(1-m)\pi(\alpha+g\omega_m+\delta_h)}{A\mu(\delta_m+\omega_m)(\alpha+\delta_h)} & \frac{b\beta(1-m)\pi(\alpha+g\omega_c+\delta_h)}{A\mu(\alpha+\delta_h)(\delta_c+\omega_c)} & \frac{b\beta(1-m)\pi(\alpha+g\omega_m+\delta_h)}{A\mu(\delta_m+\omega_m)(\alpha+\delta_h)} & \frac{b\beta(1-m)\pi(\alpha+g\omega_c+\delta_h)}{A\mu(\alpha+\delta_h)(\delta_c+\omega_c)} & \frac{b\beta g(1-m)\pi}{A\mu(\alpha+\delta_h)} \\ 0 & 0 & 0 & 0 & 0 \\ 0 & 0 & 0 & 0 & 0 \\ 0 & 0 & 0 & 0 & 0 \end{pmatrix},$$

Box I.

$$\begin{aligned} &\leq -\frac{I_m}{g}\left(1 - \frac{b\beta m\pi\left(\alpha+g\omega_m+\delta_h\right)}{A\mu\left(\delta_m+\omega_m\right)\left(\alpha+\delta_h\right)} - \frac{b\beta(1-m)\pi\left(\alpha+g\omega_c+\delta_h\right)}{A\mu\left(\alpha+\delta_h\right)\left(\delta_c+\omega_c\right)}\right) \\ &\quad -\frac{I_c}{g}\left(1 - \frac{b\beta mp\left(\alpha+g\omega_m+\delta_h\right)}{A\mu\left(\delta_m+\omega_m\right)\left(\alpha+\delta_h\right)} - \frac{b\beta(1-m)\pi\left(\alpha+g\omega_c+\delta_h\right)}{A\mu\left(\alpha+\delta_h\right)\left(\delta_c+\omega_c\right)}\right) \\ &\quad -H\left(1 - \frac{b\beta m\pi\left(\alpha+g\omega_m+\delta_h\right)}{A\mu\left(\delta_m+\omega_m\right)\left(\alpha+\delta_h\right)} - \frac{b\beta(1-m)\pi\left(\alpha+g\omega_c+\delta_h\right)}{A\mu\left(\alpha+\delta_h\right)\left(\delta_c+\omega_c\right)}\right), \\ &\leq -\frac{I_m}{g}(1-\mathcal{R}_0) - \frac{I_c}{g}(1-\mathcal{R}_0) - H(1-\mathcal{R}_0). \end{aligned}$$

When $\mathcal{R}_0 \leq 1$, $\frac{dL}{dt}$ is negative semi-definite, hence the largest compact invariant set in $\mathcal{D}$ such that $\frac{dL}{dt} = 0$ when $\mathcal{R}_0 \leq 1$ is the singleton ξ_0. By the LaSalle Invariance Principle,[15] the disease free equilibrium ξ_0 is globally asymptotically stable in $\mathcal{D}$ if $\mathcal{R}_0 \leq 1$ and unstable otherwise. □

3.3. Existence of endemic equilibrium points

To find the conditions for existence of endemic equilibrium points, let $\xi^* = \{S^*, E_m^*, E_c^*, I_m^*, I_c^*, H^*, R^*\}$ be the generic equilibrium point and $\lambda = \left(\beta b(I_c + I_m + gH)\right)/A$ be the force of infection. System (2.1) is set to zero and equilibrium point obtained in terms of the force of infection at steady state denoted as (λ^*) to satisfy the following quadratic equation.

$$C_2\lambda^{*2} + C_1\lambda^* + C_0 = 0, \tag{3.2}$$

where

$$\begin{aligned} C_0 &= -b\pi\beta\mu(\mu+\tau)\left(\omega_m\left(g\omega_c(\theta+c+e) + e\left(\alpha+\delta_h\right)\right)\right. \\ &\quad + \delta_c\left(\theta\alpha + g(\theta+c)\omega_m + \theta\delta_h + cg\delta_m\right) \\ &\quad \left.+\theta\omega_c\left(\alpha+\delta_h\right) + \delta_m\left(g(c+e)\omega_c + e\left(\alpha+\delta_h\right)\right)\right), \\ C_1 &= -\delta_m\left(\pi\alpha b\beta\left(m\tau(1-\theta-e) + (1-\theta)\tau + k_2\mu\right)\right. \\ &\quad + (\mu+\tau)\left(\omega_c\left(\alpha(-A)\mu - A\mu\delta_h + \pi b\beta g k_4\right) + \pi b\beta k_2\delta_h\right)\Big) \\ &\quad \omega_m\left(-\left((\mu+\tau)\left(\omega_c\left(-\alpha A\mu - A\mu\delta_h + \pi b\beta g\right) + \pi b\beta k_2\delta_h\right)\right.\right. \\ &\quad \left.\left.+\pi\alpha b\beta\left(k_2\mu + (1-m)\tau\right)\right)\right) \\ &\quad +\delta_c\left((\mu+\tau)\left(\delta_m(\alpha A\mu - \pi b\beta cg) + \omega_m\left(\alpha A\mu - \pi b\beta g k_3\right)\right.\right. \\ &\quad \left.\left.+ \delta_h\left(A\mu\left(\delta_m+\omega_m\right) - \pi b\beta k_1\right)\right)\right. \\ &\quad \left.-\pi\alpha b\beta(\theta(1-m)(\mu+\tau) + \mu m(1-e-c) + (1-e)m\tau)\right) \\ &\quad + \pi - b\beta\omega_c\left(k_1\delta_h(\mu+\tau) + \alpha k_1\mu + \alpha m\tau\right), \\ C_2 &= A\left(\omega_c\left(\omega_m\left(\alpha\mu + \delta_h(\mu+\tau)\right) + \delta_m\left(\delta_h(\mu+\tau) + \alpha(\mu+m\tau)\right)\right)\right. \\ &\quad \left.+\delta_c\left(\omega_m\left(\delta_h(\mu+\tau) + \alpha(\mu+(1-m)\tau)\right) + (\mu+\tau)\delta_m\left(\alpha+\delta_h\right)\right)\right), \end{aligned}$$

and

$$k_1 = m(1-\theta-e-c)+\theta, \quad k_2 = 1-\theta-c-m(1-\theta-e-c),$$

$$\begin{aligned} k_3 &= \theta + c + m(1-\theta-c-e) + \theta + c, \\ k_4 &= 1-\theta-m(1-\theta-e-c). \end{aligned}$$

In the absence of infected recruits, the parameters θ, e and c (the proportions of latently infected undetected individuals with or without comorbidity and detected infected individuals respectively recruited into a closed community) are zero. Therefore Eq. (3.2) reduces to;

$$C_2\lambda^{*2} + C_1\lambda^* = 0.$$

Clearly, $\lambda^* = 0$ is a solution and in this case, corresponding to ξ_0 and when $\lambda^* \neq 0$, the coefficient C_1 summarises as

$$C_1 = A\mu(\mu+\tau)\left(\delta_c+\omega_c\right)\left(\alpha+\delta_h\right)\left(\delta_m+\omega_m\right)\left(1-\mathcal{R}_0\right).$$

Since C_2 is always positive, then if $\mathcal{R}_0 > 1$, we have $C_2\lambda^* + C_1 = 0$ implying that $\lambda^* = -\frac{C_1}{C_2}$. In this case, a unique endemic equilibrium point (ξ_1) is obtained as given in Box II;

where

$$\begin{aligned} Q_1 &= \omega_m\left(\alpha\mu(\lambda^*+\mu+\tau) + \delta_h(\lambda^*+\mu)(\mu+\tau)\right) \\ &\quad + \delta_m\left(\alpha\mu(\lambda^*+\mu) + \delta_h(\lambda^*+\mu)(\mu+\tau) + \alpha\tau(\mu+\lambda^* m)\right), \\ Q_2 &= \omega_m\left(\alpha\mu(\mu+\tau) + \delta_h(\lambda^*+\mu)(\mu+\tau) + \alpha\lambda^*(\mu - m\tau + \tau)\right) \\ &\quad +(\lambda^*+\mu)(\mu+\tau)\delta_m\left(\alpha+\delta_h\right), \\ Q_3 &= \lambda^*(1-m)\delta_h(\mu+\tau) + \alpha(\lambda^*\mu(1-m) + \lambda^*(1-m)\tau). \end{aligned}$$

Thus, the following lemma is established.

Lemma 3.2. *The unique endemic equilibrium (ξ_1), of the "No-imported-case" model system (2.1), exists if and only if $\mathcal{R}_0 > 1$.*

Lemma 3.2 implies that COVID-19 will persist in the community even when the population is closed off for entrants. The existence of a unique endemic equilibrium also indicates the possibility of forward bifurcation where a small positive asymptomatically stable endemic equilibrium appears and the disease free equilibrium ξ_0 loses it stability. We now investigate this phenomenon using the Center Manifold Theorem,[16] and the local stability of the unique endemic equilibrium point, (ξ_1).

Re-defining the state variables $(S, E_m, E_c, I_m, I_c, H, R)$ as $(x_1, x_2, x_3, x_4, x_5, x_6, x_7)$, the associated system (2.1) is given as;

$$\begin{aligned} \frac{dx_1}{dt} &= (1-(\theta+c+e))\pi - \frac{\beta b x_1(x_3+x_4+gx_5)}{A} - \mu S + \tau R, \\ \frac{dx_2}{dt} &= f_2 = \theta\pi + \frac{m\beta b x_1(x_3+x_4+gx_5)}{A} - \rho_m x_2, \\ \frac{dx_3}{dt} &= f_3 = e\pi + \frac{(1-m)\beta b x_1(x_3+x_4+gx_5)}{A} - \rho_c x_3, \\ \frac{dx_4}{dt} &= f_4 = \rho_m x_2 - \delta_m x_4 - \omega_m x_4, \end{aligned} \tag{3.3}$$

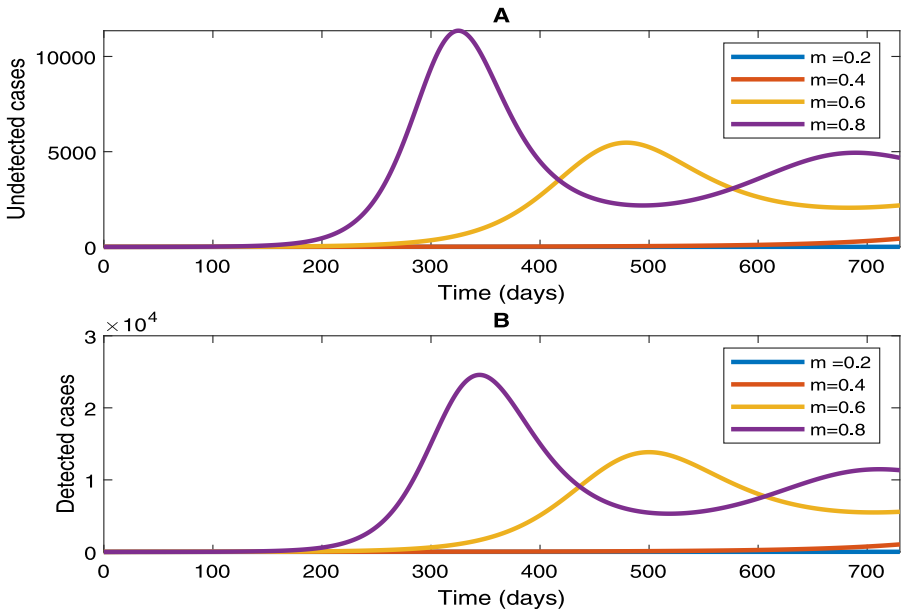

Fig. 2. Simulations of the detected and undetected SARS-COV-2 individuals with comorbidity.

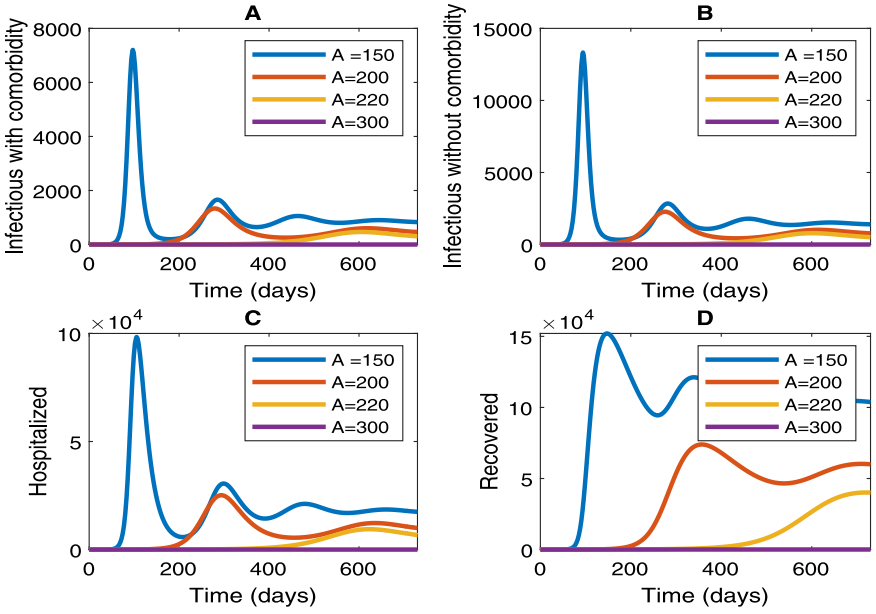

Fig. 3. Variation of the settlement area size.

$$\frac{dx_5}{dt} = f_5 = \rho_c x_3 - \delta_c x_5 - \omega_c x_5,$$
$$\frac{dx_6}{dt} = f_6 = c\pi + \omega_m x_4 + \omega_c x_5 - \delta_h x_6 - \alpha x_6,$$
$$\frac{dx_7}{dt} = f_7 = \alpha x_6 - \mu x_7 - \tau x_7.$$

The bifurcation parameter ϕ obtained by equating $\mathcal{R}_0$ to one is given in Box III. By Linearising system (3.3) at disease free equilibrium (ξ_0) and with ϕ the bifurcation parameter, we obtain

$$J_{\xi_0} = \begin{pmatrix} -\mu & 0 & 0 & -\frac{\pi b\phi}{A\mu} & -\frac{\pi b\phi}{A\mu} & -\frac{\pi b\phi g}{A\mu} & \tau \\ 0 & -\rho_m & 0 & \frac{\pi b\phi m}{A\mu} & \frac{\pi b\phi m}{A\mu} & \frac{\pi b\phi g m}{A\mu} & 0 \\ 0 & 0 & -\rho_c & \frac{\pi b\phi(1-m)}{A\mu} & \frac{\pi b\phi(1-m)}{A\mu} & \frac{\pi b\phi g(1-m)}{A\mu} & 0 \\ 0 & \rho_m & 0 & -\delta_m - \omega_m & 0 & 0 & 0 \\ 0 & 0 & \rho_c & 0 & -\delta_c - \omega_c & 0 & 0 \\ 0 & 0 & 0 & \omega_m & \omega_c & -\alpha - \delta_h & 0 \\ 0 & 0 & 0 & 0 & 0 & \alpha & -\mu - \tau \end{pmatrix}. \quad (3.4)$$

The Jacobian matrix J_{ξ_0} has zero eigenvalue and the rest are negative.

The left eigenvector associated with the zero eigenvalue of (3.4) is given by $v = (v_1, v_2, v_3, v_4, v_6, v_7)^T$ where,

$$v_1 = 0, \quad v_2 = \frac{v_6(1-\mathcal{R}_{I_c})A\mu\left(\alpha+\delta_h\right)}{gm\pi b\beta}, \quad v_3 = \frac{v_6\left(\alpha+g\omega_c+\delta_h\right)}{g\left(\delta_c+\omega_c\right)},$$
$$v_4 = \frac{v_6\left(\alpha+g\omega_m+\delta_h\right)}{g\left(\delta_m+\omega_m\right)}, \quad v_5 = \frac{v_6\left(\alpha+g\omega_{0c}+\delta_h\right)}{g\left(\delta_c+\omega_c\right)}, \quad v_6 > 0, \quad v_7 = 0. \quad (3.5)$$

Similarly, the right eigenvector of (3.4) associated with the zero eigenvalue is given by $w = (w_1, w_2, w_3, w_4, w_6, w_7)^T$, with $v.w = 1$, as shown in Box IV. Next we compute the non-zero partial derivatives of system (3.4) with respect to the state variables that are used in the computation

$$
\begin{aligned}
S_1 &= \frac{\pi(\mu+\tau)\left(\delta_c+\omega_c\right)\left(\alpha+\delta_h\right)\left(\delta_m+\omega_m\right)}{(\lambda^*+\mu)(\mu+\tau)\left(\delta_c+\omega_c\right)\left(\alpha+\delta_h\right)\left(\delta_m+\omega_m\right)-\alpha\lambda^*\tau\left((1-m)\omega_c\delta_m+\omega_m\left(m\delta_c+\omega_c\right)\right)},\\
E_{m_1} &= \frac{\pi\left(\left(\delta_m+\omega_m\right)\left(\omega_c\left(\lambda^*m\delta_h(\mu+\tau)+\alpha\lambda^*m(\mu+\tau)\right)+\delta_c\left(\lambda^*m\delta_h(\mu+\tau)+\alpha\lambda^*m(\mu+\tau)\right)\right)\right)}{\rho_m\left(Q_1\omega_c+Q_2\delta_c\right)},\\
E_{c_1} &= \frac{\pi\left(\delta_c+\omega_c\right)\left(\omega_m\left(\lambda^*(1-m)\delta_h(\mu+\tau)+\alpha\lambda^*(\mu(1-m)-m\tau+\tau)\right)+Q_3\delta_m\right)}{\rho_c\left(Q_2\delta_c+Q_1\omega_c\right)},\\
I_{m_1} &= \frac{\pi\left(\omega_c\left(\lambda^*m\delta_h(\mu+\tau)+\alpha\lambda^*m(\mu+\tau)\right)+\delta_c\left(\lambda^*m\delta_h(\mu+\tau)+\alpha\lambda^*m(\mu+\tau)\right)\right)}{Q_1\omega_c+Q_2\delta_c},\\
I_{c_1} &= \frac{\pi\left(\omega_m\left(\lambda^*(1-m)\delta_h(\mu+\tau)+\alpha\lambda^*(\mu(1-m)+(1-m)\tau)\right)+Q_3\delta_m\right)}{Q_1\omega_c+Q_2\delta_c},\\
H_1 &= \frac{\pi(\mu+\tau)\left(\lambda^*m\delta_c\omega_m+\omega_c\left(\lambda^*(1-m)\delta_m+\lambda^*\omega_m\right)\right)}{Q_1\omega_c+Q_2\delta_c},\\
R_1 &= \frac{\pi\alpha\left(\lambda^*m\delta_c\omega_m+\omega_c\left(\lambda^*(1-m)\delta_m+\lambda^*\omega_m\right)\right)}{Q_1\omega_c+Q_2\delta_c},
\end{aligned}
$$

Box II.

$$
\phi=\beta^*=\frac{A\mu\left(\delta_c+\omega_c\right)\left(\alpha+\delta_h\right)\left(\delta_m+\omega_m\right)}{\pi b\left((1-m)\delta_m\left(\alpha+g\omega_c+\delta_h\right)+\omega_m\left(g\omega_c+(1-m)\left(\alpha+\delta_h\right)\right)+m\delta_c\left(\alpha+g\omega_m+\delta_h\right)+m\omega_c\left(\alpha+\delta_h\right)\right)}.
$$

Box III.

Table 1
Parameter values used in the numerical simulations.

Parameters	Description	Values	Source
A	Settlement area size	$250\,\text{km}^2$	17
β	Transmission coefficient	$0.00056\,\text{km}^{-2}\,\text{day}^{-1}$	17
π	Constant arrival rate	$0.17\,\text{day}^{-1}$	17
μ	Per capita departure rate	$6.2\times10^{-7}\,\text{day}^{-1}$	17
g	Infectivity reduction factor among hospitalised	0.01	varied
ω_m	Hospitalisation rate of comorbidity-SARS-COV-2 individuals	$0.2\ \text{day}^{-1}$	1,6,18,19
ω_c	Hospitalisation rate of SARS-COV-2 individuals	$0.5\,\text{day}^{-1}$	1,6,18–20
c	Fraction of entrants diagnosed with SARS-COV-2	0.01	varied
θ	Fraction of undetected latently infected entrants with a comorbidity	0.1	varied
e	Fraction of undetected latently infected entrants without a comorbidity	0.1	varied
δ_h	Hospital SARS-COV-2 death rate	$0.0029\,\text{day}^{-1}$	17,19
δ_m	Death rate of undetected comorbidity-SARS-COV-2 individuals	$0.0145\ \text{day}^{-1}$	17,19
δ_c	Death rate of undetected SARS-COV-2 individuals	$0.0073\ \text{day}^{-1}$	17,19
m	Fraction of latently infected comorbidity-SARS-COV-2 individuals	0.2	varied
ρ_m	Progression of comorbidity-SARS-COV-2 individuals to infectious stage	$0.333\ \text{day}^{-1}$	18
ρ_c	Progression rate of SARS-COV-2 individuals to infectious stage	$0.25\ \text{day}^{-1}$	18
b	Fraction of susceptibles not adhering to SOPs	0.6	varied
α	Hospital recovery rate	$0.0475\ \text{day}^{-1}$	6,17,19
τ	Waning rate of disease induced immunity	$0.0083\ \text{day}^{-1}$	assumed

of coefficients **a** and **b** defined as,

$$
\mathbf{a}=\sum_{i,j,k=1}^{n} v_k w_i, w_j \frac{\partial^2 f_k}{\partial x_i \partial x_j}(0,0), \quad \text{and} \quad \mathbf{b}=\sum_{i,k=1}^{n} v_k w_i \frac{\partial^2 f_k}{\partial x_i \partial \phi}(0,0). \tag{3.7}
$$

Thus, we obtain,

$$
\begin{aligned}
&\frac{\partial^2 f_1}{\partial x_1\partial x_4}=-\frac{b\phi}{A},\quad \frac{\partial^2 f_1}{\partial x_1\partial x_5}=-\frac{b\phi}{A},\quad \frac{\partial^2 f_1}{\partial x_1\partial x_6}=-\frac{b\phi g}{A},\quad \frac{\partial^2 f_1}{\partial x_4\partial x_1}=-\frac{b\phi}{A},\\
&\frac{\partial^2 f_1}{\partial x_5\partial x_1}=-\frac{b\phi}{A},\quad \frac{\partial^2 f_1}{\partial x_6\partial x_1}=-\frac{b\phi g}{A},\quad \frac{\partial^2 f_2}{\partial x_2\partial x_4}=\frac{bm\phi}{A},\quad \frac{\partial^2 f_2}{\partial x_2\partial x_5}=\frac{bm\phi}{A},\\
&\frac{\partial^2 f_2}{\partial x_2\partial x_6}=\frac{bm\phi g}{A},\quad \frac{\partial^2 f_2}{\partial x_4\partial x_2}=\frac{bm\phi}{A},\quad \frac{\partial^2 f_2}{\partial x_5\partial x_2}=\frac{bm\phi}{A},\quad \frac{\partial^2 f_2}{\partial x_6\partial x_2}=-\frac{bm\phi g}{A},\\
&\frac{\partial^2 f_3}{\partial x_4\partial x_3}=\frac{b(1-m)\phi}{A},\quad \frac{\partial^2 f_3}{\partial x_5\partial x_3}=\frac{b(1-m)\phi}{A},\quad \frac{\partial^2 f_3}{\partial x_6\partial x_3}=-\frac{b(1-m)\phi g}{A}.
\end{aligned} \tag{3.8}
$$

The non-zero partial derivatives of system (3.3) with respect to state variables and the bifurcation parameter, ϕ are obtained as;

$$
\begin{aligned}
&\frac{\partial^2 f_1}{\partial x_4\partial\phi}=-\frac{b\pi}{A\mu},\quad \frac{\partial^2 f_1}{\partial x_5\partial\phi}=-\frac{b\pi}{A\mu},\quad \frac{\partial^2 f_1}{\partial x_6\partial\phi}=-\frac{b\pi g}{A\mu},\\
&\frac{\partial^2 f_2}{\partial x_4\partial\phi}=\frac{bm\pi}{A\mu},\quad \frac{\partial^2 f_2}{\partial x_5\partial\phi}=\frac{bm\pi}{A\mu},\quad \frac{\partial^2 f_2}{\partial x_6\partial\phi}=\frac{bm\pi g}{A\mu},\\
&\frac{\partial^2 f_3}{\partial x_4\partial\phi}=\frac{b(1-m)\pi}{A\mu},\quad \frac{\partial^2 f_3}{\partial x_5\partial\phi}=\frac{b(1-m)\pi}{A\mu},\quad \frac{\partial^2 f_3}{\partial x_6\partial\phi}=\frac{b(1-m)\pi g}{A\mu}.
\end{aligned} \tag{3.9}
$$

Substituting expressions (3.5), (3.6), (3.8) and (3.9) into Eq. (3.7) gives;

$$
\mathbf{a}=\frac{2b\beta\left((1-m)v_3w_3\left(gw_5+w_3+w_4\right)+mv_2w_2\left(gw_6+w_4+w_5\right)\right)}{A},
$$

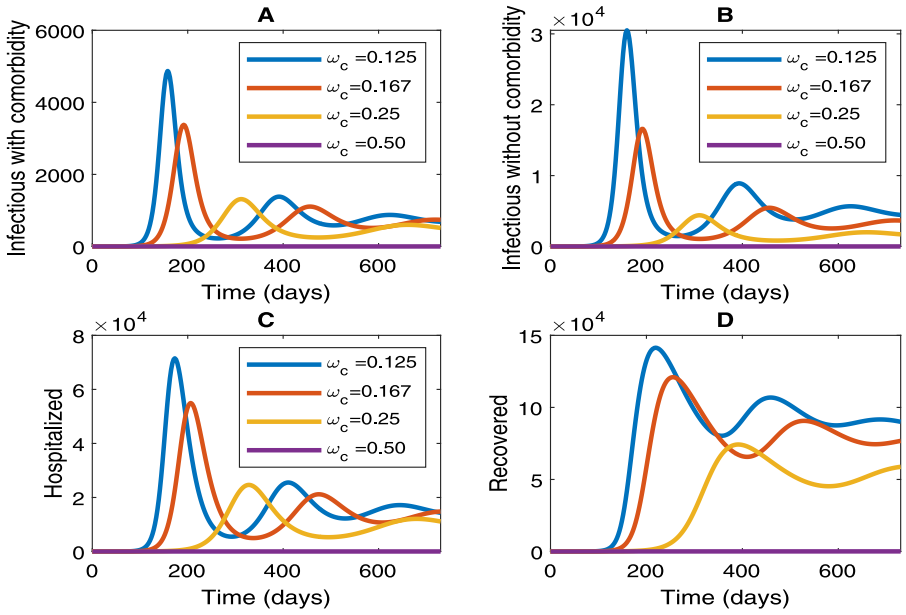

Fig. 4. Varying the hospitalisation rate of SARS-COV-2 individuals.

$$
\begin{aligned}
w_1 &= \frac{\tau w_7}{\mu} - \frac{\pi b\beta w_7(\mu+\tau)\left(A\mu\left(1-\mathcal{R}_{I_c}\right)\left(\delta_c+\omega_c\right)\left(\alpha+\delta_h\right)+\pi\alpha b\beta(1-m)\left(\alpha+g\omega_m+\delta_h\right)-Bg\right)}{\alpha AB\mu^2},\\
w_2 &= \frac{A\mu w_7\left(1-\mathcal{R}_{I_c}\right)(\mu+\tau)\left(\delta_c+\omega_c\right)\left(\alpha+\delta_h\right)\left(\delta_m+\omega_m\right)}{\alpha B\rho_m},\\
w_3 &= \frac{\pi b\beta(1-m)w_7(\mu+\tau)\left(\delta_c+\omega_c\right)\left(\alpha+g\omega_m+\delta_h\right)}{\alpha B\rho_c},\\
w_4 &= \frac{A\mu w_7\left(1-\mathcal{R}_{I_c}\right)(\mu+\tau)\left(\delta_c+\omega_c\right)\left(\alpha+\delta_h\right)}{B},\\
w_5 &= \frac{\pi b\beta(1-m)w_7(\mu+\tau)\left(\alpha+g\omega_m+\delta_h\right)}{B}, \qquad w_6 = \frac{w_7(\mu+\tau)}{\alpha},\\
w_7 &> 0, \text{ where } B = \pi\alpha b\beta(1-m)\omega_c - \alpha\omega_m\left(\pi b\beta(1-m) - A\mu\left(\delta_c+\omega_c\right)\right).
\end{aligned}
\tag{3.6}
$$

Box IV.

$$\mathbf{b} = \frac{\pi bm(v_2+v_3)(gw_3+w_4+w_5)}{A\mu}.$$

According to the Center Manifold Theorem,[16] if $B > 0$ ($\omega_c > \omega_m$) and $\mathcal{R}_{I_c} < 1$, then the coefficients $\mathbf{a} > 0$ and $\mathbf{b} > 0$. In this case, a backward bifurcation would occur but it is not possible because the absence of infected entrants into the community yields a unique endemic equilibrium. If $B < 0$ ($\omega_c < \omega_m$) and $\mathcal{R}_{I_c} < 1$, then the coefficients $\mathbf{a} < 0$ and $\mathbf{b} > 0$. In this case, the model exhibits a transcritical bifurcation at $\mathcal{R}_0 = 1$ and the "*No-imported-case*" equilibrium is locally asymptotically stable. On the contrary, if $\mathcal{R}_{I_c} > 1$, then $\mathbf{a} < 0$ and $\mathbf{b} < 0$ implying that the "*No-imported-case*" equilibrium is unstable. Therefore the following theorem is established.

Theorem 3.2. *The unique endemic equilibrium point ξ_1*

(i) is locally asymptotically stable only if $\omega_m < \omega_c$, $\mathcal{R}_{I_c} < 1$ and $\mathcal{R}_0 > 1$.
(ii) is unstable if $\omega_m > \omega_c$ and $\mathcal{R}_{I_c} > 1$.

According to Theorem 3.2, it is important for COVID-19 comorbid patients to report early for treatment and to also strictly observe SOPs since the reaped associated benefits of a significantly reduced infectious period would consequently lead to halting the spreading of the disease within the community. It is worth noting that in such a community, the disease dynamics is driven by individuals without comorbidities. Since some of these individuals are asymptomatic, they continue transmitting the disease and make its control very complicated.

3.4. Endemic equilibrium point ξ_2

Lemma 3.3. *The model system (2.1) has a unique endemic equilibrium point ξ_2 if COVID-19 infected individuals are recruited into the community.*

Proof. Suppose $\theta, e, c \neq 0$, then within a community, the endemic equilibrium point will be given by roots of polynomial (3.2). In this case, the coefficient $C_0 < 0$ and $C_2 > 0$. Therefore the only positive root of polynomial (3.2) is

$$\lambda^* = \frac{-C_1 + \sqrt{C_1^2 - 4C_2C_0}}{2C_0},$$

which gives the endemic equilibrium point shown in Box V; where

$$Q_4 = \delta_h(\mu+\tau)\left(\theta\mu + \lambda^* k_1\right) + \theta\alpha(\mu+\tau)(\mu+\lambda^*(1-m))$$

$$
\begin{aligned}
S^* &= \frac{\pi\left(\alpha\tau\left(\theta\omega_m\left(\delta_c+\omega_c\right)+\left(\delta_m+\omega_m\right)\left(c\delta_c+(c+e)\omega_c\right)\right)+k_0(\mu+\tau)\left(\delta_c+\omega_c\right)\left(\alpha+\delta_h\right)\left(\delta_m+\omega_m\right)\right)}{(\lambda^*+\mu)(\mu+\tau)\left(\delta_c+\omega_c\right)\left(\alpha+\delta_h\right)\left(\delta_m+\omega_m\right)-\alpha\lambda^*\tau\left((1-m)\omega_c\delta_m+\omega_m\left(m\delta_c+\omega_c\right)\right)},\\
E_m^* &= \frac{\pi\left(\delta_m+\omega_m\right)\left(\omega_c\left(\delta_h(\mu+\tau)\left(\theta\mu+\lambda^*k_1\right)+\theta\alpha\mu(\mu+\lambda^*(1-m)+\tau)+\alpha\lambda m(\mu(1-e-c)+\tau)\right)+Q_4\delta_c\right)}{\rho_m\left(Q_1\omega_c+Q_2\delta_c\right)},\\
E_c^* &= \frac{\pi\left(\delta_c+\omega_c\right)\left(\omega_m\left(\delta_h(\mu+\tau)\left(e\mu+\lambda^*k_2\right)+\alpha\left(e\mu(\mu+\tau)+\lambda^*\left(k_2\mu+(1-m)\tau\right)\right)\right)+Q_5\delta_m\right)}{\rho_c\left(Q_2\delta_c+Q_1\omega_c\right)},\\
I_m^* &= \frac{\pi\left(\omega_c\left(\delta_h(\mu+\tau)\left(\theta\mu+\lambda^*k_1\right)+\theta\alpha\mu(\mu+\lambda^*(1-m)+\tau)+\alpha\lambda^*m(\mu(1-c-e)+\tau)\right)+Q_4\delta_c\right)}{Q_1\omega_c+Q_2\delta_c},\\
I_c^* &= \frac{\pi\left(\omega_m\left(\delta_h(\mu+\tau)\left(e\mu+\lambda^*k_2\right)+\alpha\left(e\mu(\mu+\tau)+\lambda^*\left(k_2\mu-m\tau+\tau\right)\right)\right)+Q_5\delta_m\right)}{Q_1\omega_c+Q_2\delta_c},\\
H^* &= \frac{\pi(\mu+\tau)\left(\delta_c\left(\omega_m(\lambda^*(\theta+c+m-m(\theta+c+e))+\mu(\theta+c))+c(\lambda^*+\mu)\delta_m\right)+Q_6\omega_c\right)}{Q_1\omega_c+Q_2\delta_c},\\
R^* &= \frac{\pi\alpha\left(\delta_c\left(\omega_m(\lambda^*(\theta+c+m-m(\theta+c+e))+\mu(\theta+c))+c(\lambda^*+\mu)\delta_m\right)+Q_6\omega_c\right)}{Q_1\omega_c+Q_2\delta_c},
\end{aligned}
$$

Box V.

$$
\begin{aligned}
&+\alpha\lambda^*m(\mu(1-c-e)+(1-e)\tau),\\
Q_5 &= \alpha\left(\lambda^*\tau(1-m(-\theta-e+1)-\theta)+e\mu(\mu+\tau)+\lambda^*k_2\mu\right)\\
&+\delta_h(\mu+\tau)\left(e\mu+\lambda^*k_2\right),\\
Q_6 &= \omega_m(\mu(\theta+c+e)+\lambda^*)+\delta_m\left(\mu(c+e)+\lambda^*k_4\right). \quad \square
\end{aligned}
$$

Lemma 3.3 guarantees the possibility of an endemic equilibrium point ξ_2 and its existence reveals that the disease will persist as long as the infected individuals are continuously recruited into the community.

4. Numerical simulation results

In this Section, numerical simulations are presented to gain more insights on the model properties under various scenarios. Simulations are performed using MATLAB, version 2020a (Math Works, Inc.) software. The parameter values given in Table 1 are obtained from existing literature and some are as estimated basing on the Ugandan data.

The simulations in Fig. 2 indicate that the number of detected and undetected SARS-COV-2 cases increase with the increasing proportion of the infected individuals with a comorbidity. This is consistent with the reports of Emami et al.[21] and Bajgain et al.[22] which revealed that asymptomatic individuals with chronic underlying illnesses experience a much faster progression to the symptomatic stage as compared to individuals without any comorbidity. Results in Fig. 3 show that the infection peaks are delayed and the risk of community transmission is optimally minimised when the occupancy area is increased (based on the observation of social distancing). Therefore, policy makers should advocate for stratified settlement areas, thus reducing crowdedness through improved connectivity, where the standard operating procedures such as social distancing will easily be adhered to.

When detected cases (hospitalised patients) and undetected cases (infectious individuals with or without comorbidity) are simulated at varying levels of hospitalisation rates as exhibited in Figs. 4 and 5, it is observed that community infections grow significantly with decreasing detection rates. Conversely, increasing the hospitalisation rate (through more screening and testing of SARS-COV-2 suspects) reduces the community infection. Fig. 4 further shows that at a detection rate of $\omega_c = 0.5\,\text{day}^{-1}$ (2 days), the pandemic curve for individuals without comorbidity never peaks and remains flat implying that early detection would lead to early hospitalisation thus alleviating would be increments in community transmission. This would consequently avert overwhelming the available limited resources. Nonetheless, the simulations in Fig. 5 C suggest that maintaining the same detection rate of $\omega_m = 0.5\,\text{day}^{-1}$ for COVID-19 patients with a comorbidity would constrain the available resources since the curve peaks 3-fold higher compared to individuals without any comorbidity.

Fig. 7 D shows that when the disease spreads to COVID-19 front-line health-care workers through hospital acquired infections, the number of infected (Fig. 7 A and B) and hospitalised (Fig. 7 C) patients increases, thus stretching health-care facilities and resources. An escalation in hospital acquired infections compromises health-care services and significantly increases the doctor to patient ratio, consequently affecting the rate at which the patients recover as observed in Fig. 6 C. Overburdening of the health-care systems results into increased mortality of the SARS-COV-2 patients. Therefore, funders of health-care systems should endeavour to avail quality personal protective equipment (PPE) and put up plausible policies and strategies that would protect health-care workers from the ongoing COVID-19 pandemic.

5. Discussion

This study develops and analyses a habitat-size dependent deterministic mathematical model that is then used to gain insights into the impact of early detection and treatment on the COVID-19 epidemic curve in a community with some co-morbid individuals. The model formulated by subdividing the population into susceptible, exposed with and without comorbidities, infectious with and without comorbidities, hospitalised and recovered classes. It considers a habitat area-size dependent force of infection, whereby the transmission is based on the possibility of individuals to social distance within the community.

The solutions derived from Lyapunov stability analysis show that the model has a globally asymptomatically stable disease free equilibrium (obtained when infected individuals are denied entry to the community) whenever the basic reproduction number is less than unity. This implies that, COVID-19 can be eliminated irrespective of the initial number of infected individuals introduced in the community with some individuals having underlying health conditions. The basic reproduction number was found to be directly proportional to the infection rate, the proportion of individuals with comorbidities and those adhering to standard operating procedures and inversely proportional to the recovery rates, COVID-19 detection rates and the area size occupied by the community. Our results indicate that without infected entrants, the stability of the endemic equilibrium point when $\mathbb{R}_0 > 1$ also depends on the basic reproduction number associated with the individuals without comorbidities. It is shown that this endemic equilibrium is only locally asymptotically stable if the basic reproduction number associated with individuals without comorbidities is less than unity else it is unstable.

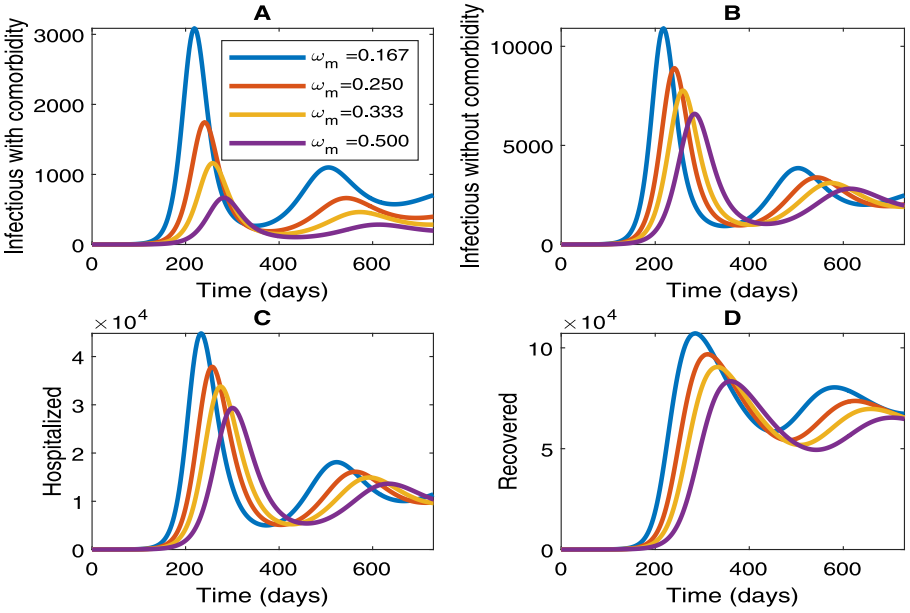

Fig. 5. Varying the hospitalisation rate of comorbidity-SARS-COV-2 individuals.

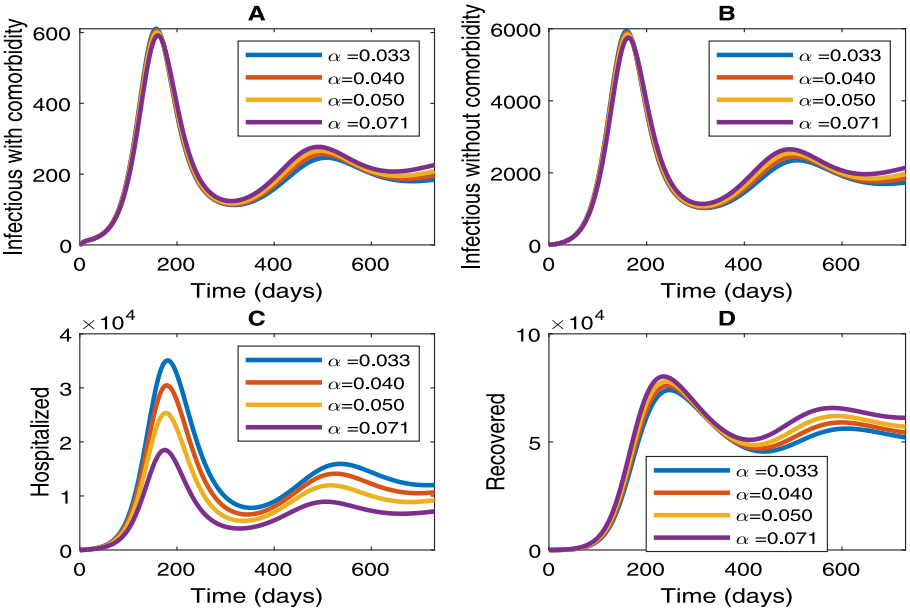

Fig. 6. Variation of hospital recovery rate.

These results reveal that as long as the individuals without comorbidities fail to observe the standard operating procedures, then COVID-19 cases especially amongst individuals with underlying conditions will increase which will overwhelm the health system.

Simulation result indicate that the number of detected and undetected cases increases with increasing proportions of individuals with comorbidity (see Fig. 2). This has been observed in several countries where there is significantly high prevalence and number of deaths as a result of comorbidities.[23] Our results in Figs. 4 and 5 further highlight the importance of early detection/reporting and effective treatment in the mitigation of COVID-19. We note that the pandemic curve remains flat when the detection/reporting rate is 0.5 amongst individuals without comorbidities. On the other hand, if only individuals with comorbidities effectively report for treatment and hospitalisation, then the epidemic curve peaks within 300 days from the pandemic outbreak, 3-fold higher amongst people without comorbidities. This implies that early detection and treatment of COVID-19 infected individuals without comorbidities would reduce on their infectiousness thus decreasing community transmissions.

In conclusion, our study emphasises adherence to standard operating procedures, early detection and treatment of COVID-19 patients especially those that do not have underlying health conditions, so as to lessen community transmission of the disease.

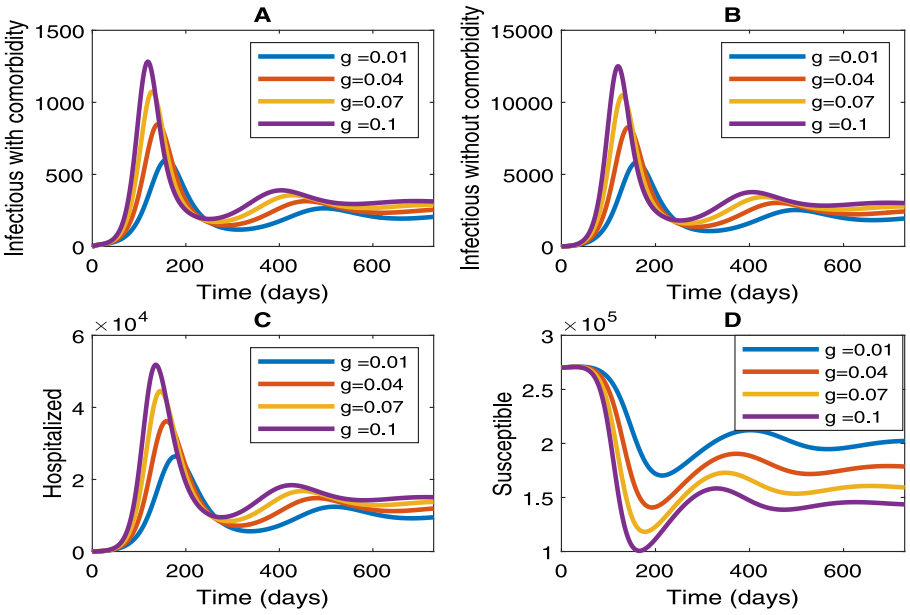

Fig. 7. Variation of hospital acquired SARS-COV-2 infection.

Declaration of competing interest

The authors declare that they have no known competing financial interests or personal relationships that could have appeared to influence the work reported in this paper.

Acknowledgements

The authors thank the Government of Uganda and Makerere University Research and Innovation Fund for the support to carry out this study, and the Ministry of Health for the data-sets on COVID-19. We also appreciate the suggested useful comments of the anonymous reviewers towards the improvement of this paper.

References

1. COVID-19 coronavirus pandemic updates. 2021 https://www.worldometers.info/coronavirus/. Accessed 29 October 2021.
2. Twahirwa Rwema JO, Diouf D, Phaswana-Mafuya N, et al. COVID-19 across Africa: Epidemiologic heterogeneity and necessity of contextually relevant transmission models and intervention strategies. *Ann Intern Med*. 2020;173(9):752–753.
3. Ye C, Zhang S, Zhang X, et al. Impact of comorbidities on patients with COVID-19: A large retrospective study in Zhejiang. *China J Med Virol*. 2020;92(11):2821–2829.
4. Bassendine MF, Bridge SH, McCaughan GW, et al. COVID-19 and comorbidities: A role for dipeptidyl peptidase 4 (DPP4) in disease severity? *J Diabetes*. 2020;12(9):649–658.
5. Richardson S, Hirsch JS, Narasimhan M, et al. Presenting characteristics, comorbidities, and outcomes among 5700 patients hospitalized with COVID-19 in the New York City area. *JAMA*. 2020;323(20):2052–2059.
6. Mugisha JYT, Ssebuliba J, Nakakawa JN, et al. Mathematical modeling of COVID-19 transmission dynamics in Uganda: Implications of complacency and early easing of lockdown. *PLoS One*. 2021;16(2):e0247456.
7. Li B, Yang J, Zhao F, et al. Prevalence and impact of cardiovascular metabolic diseases on COVID-19 in China. *Clin Res Cardiol*. 2020;109(5):531–538.
8. Marimuthu Y, Nagappa B, Sharma N, et al. COVID-19 and tuberculosis: A mathematical model based forecasting in Delhi India. *Indian J Tuberc*. 2020;67(2):177–181.
9. Simonnet A, Chetboun M, Poissy J, et al. High prevalence of obesity in severe acute respiratory syndrome Coronavirus-2 (SARS-CoV-2) requiring invasive mechanical ventilation. *Obesity (Silver Spring)*. 2020;28(7):1195–1199.
10. Thomas DM, Sturdivant R, Dhurandhar NV, et al. A primer on COVID-19 mathematical models. *Obesity (Silver Spring)*. 2020;28(8):1375–1377.
11. Omame A, Sene N, Nometa I, et al. Analysis of COVID-19 and comorbidity co-infection model with optimal control. *Optim Control Appl Meth*. 2021:1–13.
12. Kirkcaldy RD, King BA, Brooks JT. COVID-19 and postinfection immunity: Limited evidence, many remaining questions. *JAMA*. 2020;323(22):2245–2246.
13. Lakshmikantham V, Leela S, A.A. Martynyuk. *Stability Analysis of Nonlinear Systems*. New York: M. Dekker; 1989.
14. van den Driessche P, Watmough J. Reproduction numbers and sub-threshold endemic equilibria for compartmental models of disease transmission. *Math Biosci*. 2002;180:29–48.
15. La Salle JP. *The Stability of Dynamical Systems*. Society for Industrial and Applied Mathematics; 1976.
16. Castillo-Chavez C, Song B. Dynamical models of tuberculosis and their applications. *Math Biosci Eng*. 2004;1(2):361–404.
17. Government of Uganda/UN high commissioner for refugees (2019) Uganda - Refugee statistics - Bidibidi. 2020 https://reliefweb.int/report/uganda/uganda-refugee-statistics-april-2019-bidibidi. Accessed 10 November 2020.
18. Wu JT, Leung K, Leung GM. Nowcasting and forecasting the potential domestic and international spread of the 2019-nCoV outbreak originating in Wuhan, China: a modelling study. *Lancet*. 2019;395(10225):689–697.
19. Ssematimba A, Nakakawa JN, Ssebuliba J, et al. Mathematical model for COVID-19 management in crowded settlements and high-activity areas. *Int J Dyn Control*. 2021:1–12.
20. Lin Q, Zhao S, Gao D, et al. A conceptual model for the coronavirus disease 2019 (COVID-19) outbreak in Wuhan, China with individual reaction and governmental action. *Int J Infect Dis*. 2019;93:211–216.
21. Emami A, Javanmardi F, Pirbonyeh N, et al. Prevalence of underlying diseases in hospitalized patients with COVID-19: a systematic review and meta-analysis. *Arch Acad Emerg Med*. 2020;8(1):e35.
22. Bajgain KT, Badal S, Bajgain BB, et al. Prevalence of comorbidities among individuals with COVID-19: A rapid review of current literature. *Am J Infect Control*. 2021;49(2):238–246.
23. Kyrychko YN, Blyuss KB, Brovchenko I. Mathematical modelling of the dynamics and containment of COVID-19 in Ukraine. *Sci Rep*. 2020;10:19662.